Corrosion performance of thermally sprayed aluminium (TSA) in simulated deep sea environment

Shiladitya PAUL[1]

[1]*Materials Group, TWI, Cambridge, UK, Shiladitya.Paul@TWI.co.uk*

Abstract:
Thermally sprayed aluminium (TSA) has been used in offshore applications for decades. Their effectiveness in mitigating corrosion of offshore steel structures has been proven over the years. However, very little work is reported on the performance of TSA when damaged. Furthermore, data on the performance of damaged TSA in deep sea is virtually non-existent. The paper addresses this knowledge gap and reports the corrosion performance of damaged TSA on carbon steel in a simulated deep sea environment. Holiday (artificially induced defect) amounting to 3% of the sample area was drilled to expose the underlying carbon steel and the sample was exposed to synthetic seawater at 5°C for 30 days in an autoclave at 50 MPa to simulate 5000 m of water depth. After testing, examination of the sample revealed the formation of calcareous deposit on the exposed steel surface with no visible steel corrosion product. Detailed microstructural characterisation of the calcareous deposit confirmed the formation of protective Mg-based layers. This elucidates that TSA has the ability to protect carbon steel in simulated deep sea environment even when damaged.

Keywords: thermally sprayed aluminium; deep sea; damaged TSA; marine corrosion;

Introduction

It is well established that thermally sprayed aluminium (TSA) coatings provide long-term corrosion protection of offshore steel structures [1, 2]. The low corrosion rate of TSA coupled with its ability to act as an anodic coating makes it ideal for such applications [3-5]. This anodic nature of aluminium offers sacrificial protection to carbon steel in seawater resulting in the formation of calcareous deposits on any exposed steel [6]. Such deposits have the favourable effect of reducing the cathode area and hence decreasing the corrosion rate [7].

Performance of TSA in protecting steel in marine environments has been widely investigated in long-term laboratory as well as on-site studies [2, 8-10]. It is known that TSA has the ability to polarise steel in seawater and provide a substantial level of cathodic protection at ambient and elevated temperatures, even when damaged [5-7]. The behaviour of TSA on steel in seawater with and without external cathodic protection has also been explored [5]. Additionally, work has been carried out to study the mechanism of calcareous deposit formation in seawater [4, 9-11]. The influence of parameters, such as temperature, pH and various ions present in seawater has been studied. Although, several papers have been published in the area, the research so far on calcareous deposits formation has focussed on ambient pressure exposure, typically at ambient temperatures with applied potential, not TSA coatings.

It must be noted that the application of TSA in the offshore environment is not limited to ambient conditions. For deep subsea pipelines where the temperature is low in most cases and the external hydrostatic pressure is usually high (depending on depth), the rate of formation of calcareous deposit and its composition may differ. The nature of the calcareous deposit: its density, barrier property, friability, adherence and overall integrity in deep sea environments in unknown. This missing information is crucial as deep subsea pipelines may be in contact with the rough seabed where the erosion and wear is likely.

This paper addressed part of the above mentioned technology gap. Arc-sprayed aluminium-coated carbon steel samples with controlled defect (holiday) were exposed to synthetic seawater at 5°C for 30 days in an autoclave at 50 MPa (500 bar) to simulate 5000 m of water pressure to study the protective performance of TSA.

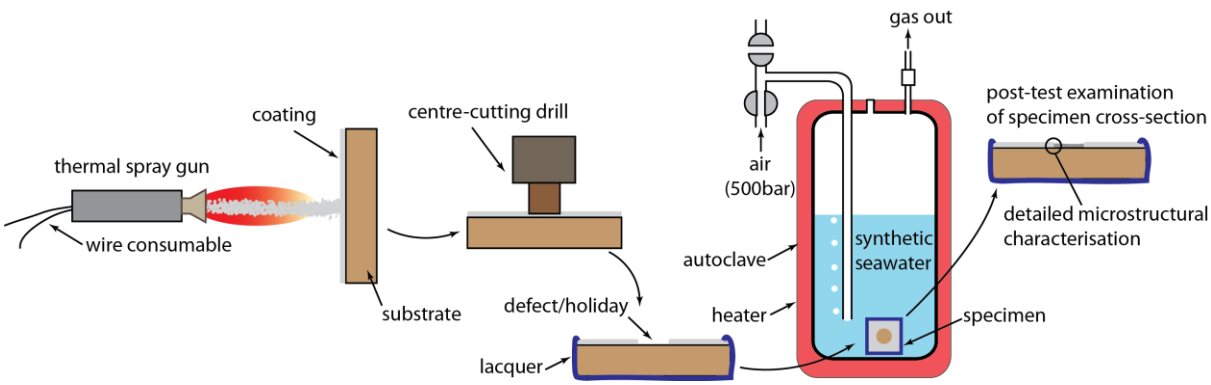

Figure 1: *Schematic showing the various operations undertaken in the experimental work*

Experimental

General Remarks

The experimental work involved thermal spraying, creation of defects, preparation of specimens for exposure tests, exposure to synthetic seawater at 50 MPa under air for 30 days and post-test characterisation. The operations undertaken in shown in a schematic (Figure 1).

Materials

Carbon-Manganese steel often used in offshore environments, conforming to specification S355J2+N(2004), was selected as the substrate material. The coating material was 2.3mm diameter commercially 'pure' aluminium (99.5% Al) supplied by Metallisation Ltd. (UK). The nominal composition of the substrate and coating material (wire consumable) is given in Table 1.

Table1: *Composition of steel substrate and aluminium wire consumable (coating material)*

Materials	Element (wt.%)							
	C	Mn	Si	S	P	Fe	C	Al
S355 Steel (Substrate)	0.12	1.39	0.39	0.019	0.014	Bal..	-	-
Al wire (consumable)	-	<0.01	0.07	-	-	0.21	<0.01	Bal.

Coating Production

The substrate in plate form was cut into 42 mm×40 mm×6 mm flat panels and the edges were rounded off using a file prior to further preparation. Prior to coating, the substrates coupons were degreased and then prepared by blasting with F60 and NK12 alumina grit to give a rough surface to which the molten and semi-molten spray particles can key onto.

Thermal spray coatings were prepared using a Metallisation 528 twin wire arc spray gun mounted on a 6-axis robot. Dry compressed air, supplied at 5.5bar, was used as the particle atomising and propellant gas. Coatings were produced on one surface using the spray parameters given in Table 2 to attain a nominal coating thickness of 300µm.

Table2: *Spray parameters used to prepare TSA coatings*

Make/Gun	Wire feed rate (g min^{-1})	Stand-off distance (mm)	Increment step (mm)	Traverse speed (m s^{-1})	Air pressure (MPa)
Metallisation 528	98.7	95	15	0.5	0.55

Sample Preparation

TSA-coated specimens were taken and an 8 mm diameter slot drill was used to remove the coating to expose the steel substrate (~3% area of the coating surface). The side and edges of the specimens were covered with a curable polymer to protect the surfaces not intended to be exposed. The exposed TSA surface area was 15.5 cm^2 (obtained by taking the holiday area into account).

Testing in a High Pressure Autoclave

A glass-lined high pressure autoclave designed to operate at 75 MPa was used for the immersion test. Specimen was placed in the autoclave cooled to 5°C and 400mL of chilled synthetic seawater (ASTM D1141) was poured into it [12]. The autoclave was pressurised to 50 MPa (500 bar) by compressed air and kept at pressure for 30 days.

Determination of Corrosion Rates

The corrosion rate (CR) was calculated by noting the amount of dissolved aluminium in seawater after testing. As no aluminium (Al) or iron (Fe) salt is present in ASTM D1141 synthetic seawater, all Al^{3+} ions (y mg L^{-1}) and Fe^{3+} ions (z mg L^{-1}) present after testing must have come from the TSA coating. Since the volume of solution used is known (0.4 L), we can calculate the amount of Al and Fe lost from the surface of the coating in 30 days by taking the density of Al (2.70 g cm^{-3}) and Fe (7.85 g cm^{-3}) into account.

Volume of Al lost from the sample = 0.4y/2700 cm^3

Volume of Fe lost from the sample = 0.4z/7850 cm^3

The amount of Al^{3+} in solution was converted to the thickness of TSA lost during exposure (d_{Al} mm) by noting the geometric area of the coating exposed (15.5cm^2). This was found to be:

d_{Al} (or CR_{Al}) = 4y/(2700×15.5) mm in 30 days, or

d_{Al} (or CR_{Al}) = 4y×365.25/(2700×15.5×30) mm y^{-1}

Similarly, from the exposed steel area the amount of Fe^{3+} in solution was converted to the thickness of TSA lost during exposure (d_{Fe} mm) by noting the geometric area of the steel exposed (area corresponding to a 8 mm defect = 0.5cm^2). It was assumed that the dissolved Fe has only come from the artificially induced defect region and not from anywhere else. The corrosion rate was found to be:

d_{Fe} (or CR_{Fe}) = 4z/(7850×0.5) mm in 30 days, or

d_{Fe} (or CR_{Fe}) = 4z×365.25/(7850×0.5×30) mm y^{-1}

Microstructural Characterisation

After the autoclave exposure the specimen was taken out, dried and photographed. The surfaces of the corroded specimen were examined by light optical microscopy and SEM (specimen was gold coated prior to this), including element mapping obtained using energy dispersive X-ray spectroscopy (EDX). Further analysis of cross-sections was also carried out to understand the corrosion mechanism.

Results

Specimen surface

The samples were photographed before and after exposure to synthetic seawater, Figure 2. The exposed steel in the defect or holiday region did not show any rust, Figure 2. The presence of white corrosion product is evident on the surface of the TSA coating, Figure 2b. White deposit is also seen in the holiday region on the surface of exposed steel (Figure 2c).

The curable polymer used to protect the edges and the back surface of the specimen performed well and no rust or corrosion product was seen in these regions.

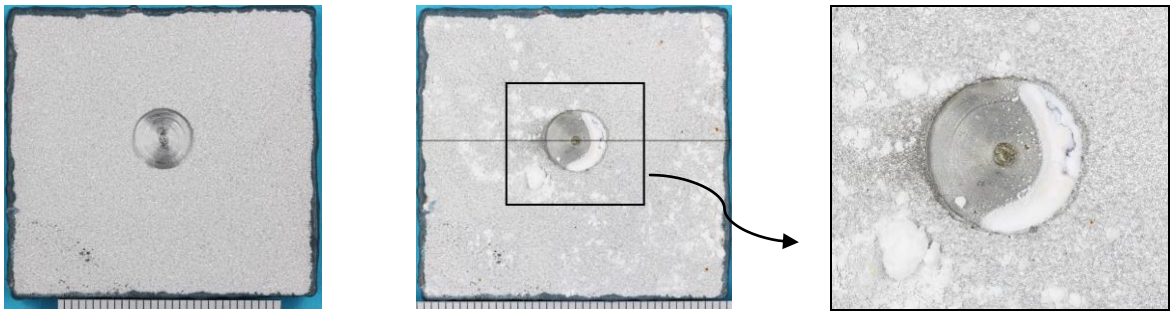

(a) (b) (c)

***Figure 2**: Photographs of samples before (a) and after (b) testing in synthetic seawater. The exposed steel region is also shown (c). The line in (b) shows the region along which the specimen was sectioned for further analysis.*

The white powdery deposit distributed randomly on the surface of the TSA coating after exposure was analysed using a SEM/EDX, Figure 3. The reason for this uneven distribution is not entirely clear. However, the length-scale and distribution of porosity in thermal spray coatings is difficult to predict and this will be invariably linked to the corrosion behaviour. It is likely that TSA in the regions with interconnected porosity corrode more to protect the underlying steel, giving more white corrosion product when the solubility limit of the corrosion product is exceeded.

The SEM micrograph shows light and slightly dark regions in the deposit in the electron back scattered mode (Figure 3a). The EDX spectra of the white spots (light regions) showed Al and O (amongst other elements such as S, Cl and Na present in seawater), implying the presence of oxide and possibly hydrated oxides of aluminium, Figure 3b. The darker regions also had very similar EDX patterns (not shown). The reflectivity of the coating also changed i.e. metallic lustre offered by TSA when sprayed was lost after exposure due to the generation of a corrosion product layer on the TSA surface, as expected.

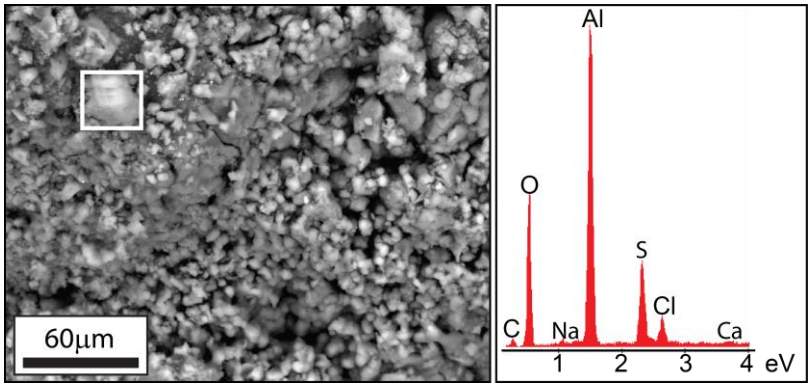

(a) (b)

***Figure 3**: SEM micrograph of the surface of the coating showing the white deposit (a) and the associated EDX pattern for the highlighted region (b).*

Microstructural characterisation of specimen cross-section

Detailed microstructural examination of cross-section of the artificially introduced defect or holiday region revealed the formation of a thick scale covering part of the steel surface, Figure 3. The machined holiday was deep enough to cut through the entire thickness of the coating. The thickness of deposit formed on the exposed steel surface was up to 1.2 mm in places. The deposit appeared to be porous in places with some dense regions. The growth of the deposit in some places were high which meant that part of the TSA was covered, Figure 4. The contrast in the back-scattered electron (BSE) mode can be observed which indicates the presence of different chemical constituents. The white regions (e.g. region 1 in Figure 4) are expected to have different chemical composition from the slightly darker regions (e.g. region 2). Three regions were selected based on the BSE image contrast. These were marked as regions 1, 2 (Figures 4 and 5), and 3 (Figure 6).

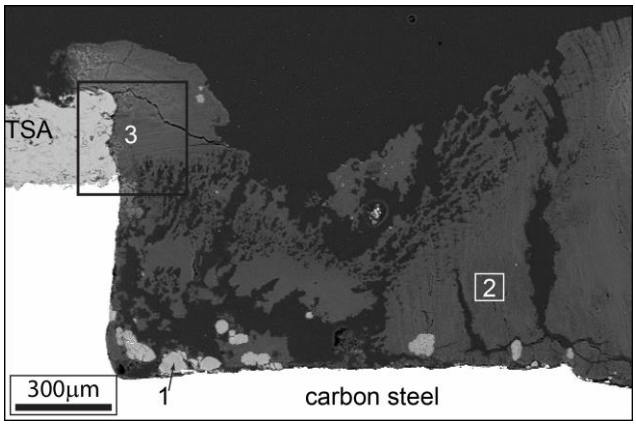

***Figure 4**: TSA-coated specimen tested in synthetic seawater at 5°C showing SEM image of cross-section along the holiday.*

On closer examination of the deposit using EDX, it was observed that the darker coloured layer (region 2 in Figure 4) predominantly contained Mg and O indicating the possible presence of $Mg(OH)_2$), Figure 5. The other elements present were Ca, Cl, Au and C possibly from seawater (Ca, Cl) or as a result of the sample preparation process (Au, C). The white areas (region 1 in Figure 4) predominantly contained Ca, with some Mg, O and C. The C seen could possibly be due to the ingress of the carbonaceous mounting resin or due to the formation of a carbonate. Due to the small, scattered volume of the white deposit no x-ray diffraction was carried out to analyse the crystalline phases present.

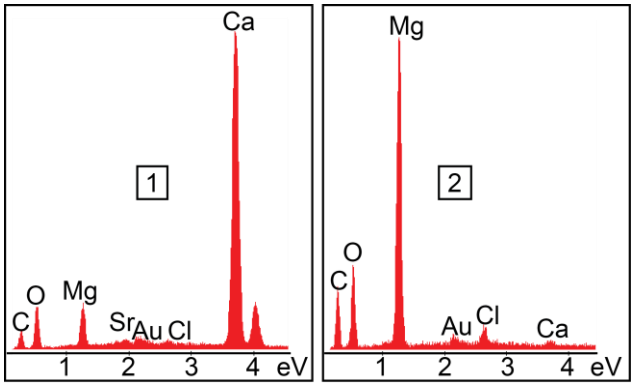

***Figure 5**: TSA-coated specimen tested in synthetic seawater at 5°C showing EDX traces of regions 1 and 2.*

The region close to the TSA layer when analysed in detail showed two different types of deposits/corrosion products (Figure 6). The difference in the composition within the TSA is also apparent. The different colours are possibly due to the presence of oxides within the TSA layer. These oxides could be the result of (i) the oxidation during the spray process and/or (ii) corrosion due to surface-connected porosity. Some cracks were also seen in the deposit close to the TSA layer. The interface between TSA and layer '(A)' had different composition to the layer further away from it, '(B)'. The EDX pattern of layer A showed the presence of Al, Mg, O, C, Na, Au and Ca. Of these, the presence of Al and O indicates the presence of alumina and/or hydrated alumina on TSA. However, the composition of the 'B' layer was different and did not show much Al. It was predominantly a Mg-containing compound. This layer seems to have the same composition as the deposit formed on the exposed steel surface away from the TSA layer.

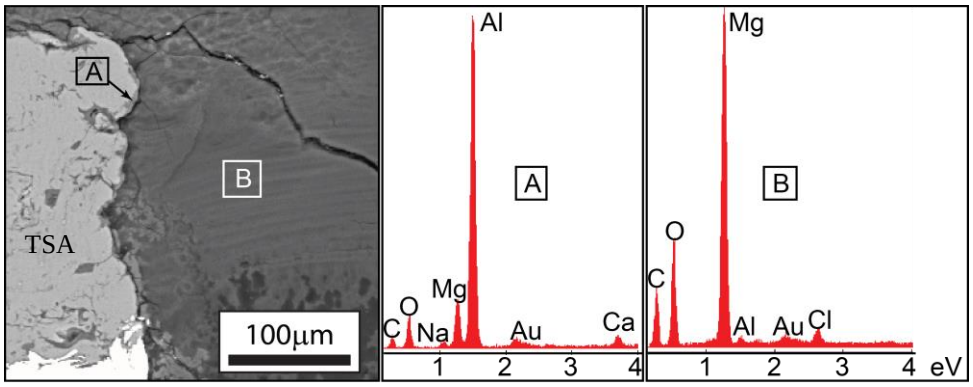

***Figure 6**: Higher magnification SEM image of region 3 (from Figure 4) showing the EDX patterns of regions A and B.*

Corrosion rate

The amount of dissolved Al and Fe were found to be 12.93 mg L^{-1} and 0.12 mg L^{-1}, respectively. Taking the density of Fe and Al, and the surface areas exposed the dissolution rate was converted to a corrosion rate of 0.015 mm y^{-1} for Al and 0.0015 mm y^{-1} for carbon steel. These numbers are approximate values as the extrapolation of corrosion rate from short-term tests to a long-term corrosion rate is prone to propagation of errors. Nonetheless, the negligible loss of Fe from carbon steel in seawater elucidates the sacrificial protection offered to steel by TSA in seawater.

Discussion

Corrosion of TSA in seawater

Copper-free aluminium alloys are generally resistant to natural seawater. The corrosion mechanism of aluminium is considered to be the one of localized attack (i.e., pitting) as opposed to uniform or general corrosion [16]. Therefore, corrosion rate calculated from weight change can be misleading as this requires the assumption that the material is lost uniformly from the exposed surface. Rates of pitting usually range from 3 to 6 µm y^{-1} during the first year and from 0.8 to 1.5 µm y^{-1} averaged over a 10-year period [17]. These values are different from the ones presented here ~15 µm y^{-1}. The difference arises due to various contributing factors. The work reported here is on TSA and not monolithic Al block. Further, damage was introduced in TSA where carbon steel, a material cathodic to Al in seawater, was exposed. This is likely to accelerate the corrosion of Al which was assumed to be of the type-general corrosion to calculate a corrosion rate. No attempt was made to measure pit depth as

the rough surface of TSA would make such attempt futile. The short test duration of 30 days is not considered long enough to give the long-term performance of these coatings. The long-term tests usually give lower corrosion rates owing to the tendency of the older pits to become inactive or the passivation of Al to occur. Another factor to consider is the pressure at which the tests were carried out. There are no reported corrosion rate values at 5 km depth in seawater. Limited information on the corrosion behaviour of aluminium alloys in deep seawater suggests that the behaviour is very similar to that at the surface except that the effect of crevices is greater [17].

Mechanism of protection offered by TSA to steel even when damaged

The morphology of the calcareous deposits formed on a cathodically polarised steel surface is temperature dependent [7]. At low temperatures (≤5°C), Mg-rich deposit is reported at ambient pressures, but at ambient temperatures (20-25°C) and ambient pressures Ca-rich deposits are formed, presumably due to the difference in the temperature dependence of the solubility limits of $Mg(OH)_2$ and $CaCO_3$ [6, 13]. Solubility of $CaCO_3$ in water decreases while that of $Mg(OH)_2$ increases with increasing temperatures. For precipitation, supersaturation is essential and supersaturation of $Mg(OH)_2$ can arise near the steel surface as a consequence of the production of OH^-. The generation of OH^- can also affect the solubility of Ca^{2+}, especially in the presence of dissolved CO_2 (which affects the calco-carbonic equilibrium).

The steel-seawater interface has a pH possibly above 9.2 (calculated at 18-20°C) which allows the precipitation of $Mg(OH)_2$. As the $Mg(OH)_2$ precipitates at the interface, the pH decreases away from the interface to a value where $Mg(OH)_2$ can no longer precipitate. Packter and Derry [14], and later Yang et al. [15] demonstrated that $Mg(OH)_2$ can co-precipitate with iron hydroxides. The pH at which this can occur was calculated to be ~2.3 [15], well below the pH at which precipitation of $CaCO_3$ can ensue. Hence, the deposit predominantly consists of $Mg(OH)_2$ close to steel with some specks of $CaCO_3$, sometimes embedded in the $Mg(OH)_2$ precipitate, Figure 7.

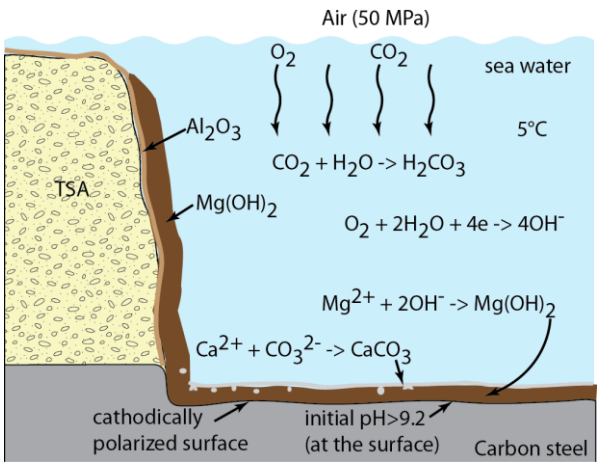

***Figure 7**: Mechanism of calcareous deposit formation on steel surface polarised by TSA in seawater containing dissolved air at 5°C*

The galvanic series of materials in seawater gives a good indication regarding the anodic and cathodic behaviour of materials when in electrical contact. Aluminium being more electronegative or active to carbon steel acts as an anode when arc-sprayed. Aluminium being anodic to carbon steel in seawater protects it by being preferentially consumed, thus providing

cathodic protection. Owing to this nature, Al is thermally sprayed onto carbon steel to protect offshore steel structures from the corrosive seawater. The environment includes splash and tidal zones and submerged structures. Although, aluminium is anodic to steel, the primary function of the coating is to act as a barrier. This is the reason why it can protect steel in areas where a continuous layer of electrolyte is not present such as in the splash and tidal zones. If the barrier is breached, the anodic nature of the coating becomes vital. Even in the absence of an external damage thermally sprayed coatings contain porosity as a result of the spraying process. The molten and semi-molten droplets of Al impinge on the substrate and form the coatings by overlapping pancake-shaped splats. As the droplets impinge they form inter-splat pores and the cooling also causes shrinkage pores. Some of the internal pores are surface-connected and at times reach the substrate. The presence of surface-connected porosity (or through porosity) could result in the electrolyte (seawater) reaching the substrate, but since the substrate (steel) is cathodic to the coating (anode), corrosion of steel is not expected. Al will dissolve while protecting the steel substrate from corrosion. However, there will be some corrosion of steel which is often negligible. The rate of corrosion of steel will depend on, amongst other factors, the area of steel exposed, temperature, dissolved oxygen content, conductivity of the electrolyte etc.

The anode (Al in the case of TSA-coated steel) while protecting the steel polarises the exposed surface and this polarisation facilitates the cathodic reaction on the steel surface results in the production of hydroxyl ions (OH^-), which increases the interfacial pH. The generation of OH^- occurs either due to the reduction of dissolved oxygen or by the reduction of water (which occurs at slightly greater negative potential) [9, 11]. The generation of OH^- ions facilitates the precipitation of magnesium hydroxide from seawater. Moreover, the increased production of OH^- leads to changes in the stability of dissolved Ca^{2+} ions at the steel surface. The Ca^{2+} ions form the basis of calco-carbonic equilibrium which is governed by the dissolution and subsequent dissociation of CO_2 in seawater. The use of pressurized air in synthetic seawater to simulate deep sea environments can be questioned as the dissolved oxygen (DO) content in the test will be higher than that observed in reality. At ambient conditions the DO content in oxic surface seawater is 6-8 mL L^{-1}. This can be significantly different in subsea environments where the oxygen minimum zones can have DO below 0.1 mL L^{-1} [18].

It is generally recognised that during subsea cathodic protection, the formation of calcareous deposit on exposed steel surface is favourable since it reduces the cathode area. These deposits on steel under cathodic protection comprises $CaCO_3$ and $Mg(OH)_2$ at ambient seawater temperatures [5-7]. The solubilities of the components of the calcareous deposit imply that predominantly $Mg(OH)_2$ will be deposited at 5°C in synthetic seawater kept at 50 MPa (500 bar), very similar to observations at similar temperatures, but at ambient pressures. However, the formation of calcareous deposit and the subsequent reduction in the corrosion of exposed steel is in line with the observation of previous experimental work where an increase in exposure time resulted in a reduction in corrosion rate with time [6].

Conclusions

The following conclusions can be drawn from this work where damaged TSA was used to understand the mechanism of corrosion protection offered by TSA in a simulated deep sea environment at 5°C:

- TSA protected the exposed steel (~3% area) from seawater and no rust was seen in the artificially induced defect (holiday region).

- The calculated corrosion rate extrapolated from the 30 day test data was found to be 0.015 mm y^{-1} for Al and 0.0015 mm y^{-1} for carbon steel.
- The low corrosion rate and high integrity of TSA implies that it can provide long-term corrosion protection to carbon steel offshore structures in deep sea environments. The anodic nature of TSA also ensures the protection of steel even when TSA is damaged in certain regions.

Acknowledgements

The work was funded by TWI. The author would like to thank TWI staff, especially Ian Wallis, Andrew Tabecki and Sheila Stevens for their technical support.

References

1 S. Paul, "Corrosion control for marine- and land-based infrastructure applications", ASM Handbook, Vol. 5A, pp. 248-252, ASM International, Ohio, 2013.
2 S. Kuroda et al., Corrosion, **62** (2006), Issue 7, pp. 635-647.
3 S. Paul et al., "Corrosion testing of thermally sprayed aluminium", ITSC 2015, paper no. 38552 (Long Beach, CA: ASM International, 2015), pp 964-970.
4 S. Paul et al., Journal of Thermal Spray Technology, **22** (2013), Issue 2-3, pp328-336.
5 P. O. Gartland and T.G. Eggen, "Cathodic and anodic properties of thermally sprayed Al- and Zn-based coatings in seawater", Corrosion 1990, paper no. 367 (Houston, TX: NACE, 1990), pp. 1-16.
6 S. Paul et al., "Electrochemical monitoring of thermally sprayed aluminium coatings on steel in a simulated marine immersion environment", Eurocorr 2014, Paper No 7458, (Pisa, Italy: EFC, 2014), pp. 1-7.
7 S. Paul, Thermal Spray Bulletin, **8** (2015), Issue 2, pp. 139-146.
8 K. Fischer et al., Materials Performance, **34** (1995), No. 4, pp. 27-35.
9 C. Rousseau et al., Corrosion Science, **52** (2010), No. 6, pp. 2206-2218.
10 R. M. Kain and E.A. Baker, "Marine atmospheric corrosion museum report on the performance of thermal spray coatings on steel", ASTM Report STP 947 (Philadelphia, PA: ASTM, 1987), pp. 211.
11 C. Barchiche et al., Eletrochimica Acta, **49** (2004), Issue 17-18, pp. 2833-2839.
12 ASTM D1141-98(2013), "Standard Practice for the Preparation of Substitute Ocean Water", ASTM International, West Conshohocken, PA, 2013.
13 M. M. Kunjapur et al., Corrosion, **43** (1987), No. 11, pp. 674-679.
14 A. Packter and A. Derry, Crystal Research and Technology, **21** (1986), No. 11, pp. 1391-1400.
15 Y. Yang et al., Metals, **5** (2015), pp. 439-56.
16 K. F. Lorking and J.E.O. Mayne, Journal of Applied Chemistry, **11** (1961), No. 5, pp. 170-180.
17 E. Ghali, "Aluminum and Aluminum Alloys", in Uhlig's Corrosion Handbook, 3rd Edition (Ed. R. W. Revie), pp. 715-745, John Wiley & Sons, Hoboken, NJ, USA, 2011.
18 L. A. Levin, American Scientist, **90** (2002), pp. 436-444.